# ELECTROCHEMICAL INVESTIGATIONS OF THE NICKEL(II)–PENICILLAMINE SYSTEM. 2. DIRECT IDENTIFICATION OF COMPLEX SPECIES INVOLVED IN CATALYTIC NICKEL REDUCTION ON THE DROPPING MERCURY ELECTRODE*

Florinel G. BANICA[a] and Ana ION[b]

[a] *Department of Chemistry (Rosenborg), Norwegian University of Science and Technology, N-7034 Trondheim, Norway; e-mail: f.banica@chembio.ntnu.no*

[b] *Department of Analytical Chemistry and Instrumental Analysis, Polytechnical University of Bucharest, Calea Grivitei 132, 78 122 Bucharest, Romania; e-mail: ana_ion@chim.upb.ro*

Received February 27, 1998
Accepted May 29, 1998

*Dedicated to Dr Aurelian Calusaru on the occasion of his 70th birthday.*

The catalytic polarographic nickel prewave was investigated by making appropriate correlations between prewave current and complex species concentrations as calculated by means of available formation constants. It was concluded that the active species is (D-penicillaminato-*N*,*S*)nickel(II) [NiL], whereas the bis-ligand complex, $[NiL_2]^{2-}$, is inert and does not play any role in the electrode process. The catalytic character of the electrode process originates from the regeneration of [NiL] by the reaction of adsorbed ligand molecules with free nickel ions available in the bulk of the solution. Conversely, all the complex species in the $Ni^{2+}$–cysteine system are labile. Consequently, the reaction mechanism in this case may include the dissociation of the complex $[NiL_2]^{2-}$ as an alternative path for the generation of the active species, [NiL]. The bell-shaped form of the prewave was interpreted in terms of potential-dependent catalyst adsorption.

**Key words**: Catalytic currents; Penicillamine; Nickel complexes; Cysteine; Polarography; Electrochemistry; Amino acids; Chelates.

D-Penicillamine ($(CH_3)_2C(SH)CH(NH_3^+)COO^-$, $H_2L$, further abbreviated as Pen) forms strong complex compounds with transition metal ions[2]. This property is the basis of various medicinal applications including $Ni^{2+}$ detoxication[3]. In a recent paper[1] it was shown that the species $[NiL_2]^{2-}$ is kinetically inert and not reducible on the dropping mercury electrode whereas the minor species [NiL] is electrochemically active. The above conclusion was derived from the investigation of the penicillamine effect on the

* Part 1: see ref.[1].

nickel polarographic diffusion wave. In this paper, the polarographic reduction of [NiL] species in the region of the catalytic nickel prewave (CNP) is examined. This is a continuation of the previous investigations on the CNP induced by cysteine[4–7], selenocysteine[8], cysteinyl dipeptides[9] and glutathione[10,11]. As compared to the above compounds, Pen shows the unique advantage of forming only two complexes with $Ni^{2+}$ ([NiL] and $[NiL_2]^{2-}$) whereas the polynuclear species are absent (ref.[1] and references therein). Therefore, it is possible to make a direct correlation between the CNP current and the concentration of the complex species calculated by means of equilibrium data. This approach is applied in this paper using the equilibrium constants reported in ref.[12], *i.e.*, log $\beta_{11}$ = 10.749, log $\beta_{12}$ = 22.886, p$K_2$ = 10.679, p$K_3$ = 8.035. Here $\beta_{11}$ and $\beta_{12}$ stand for formation constants of [NiL] and $[NiL_2]^{2-}$, respectively, $K_2 = [HL^-][H^+]/[H_2L]$ and $K_3 = [L^{2-}][H^+]/[HL^-]$, where $[HL^-]$ denotes the sum of the concentrations of $(CH_3)_2C(S^-)CH(NH_3^+)COO^-$ and $(CH_3)_2C(SH)CH(NH_2)COO^-$. In this way, it was possible to draw some general conclusions about the stoichiometry of the catalytic nickel reduction in the presence of cysteine-like ligands. This topic was recently related to biomimetic chemistry of nickel[13] and the electrochemical simulation of the nickel center behaviour in hydrogenase[14]. The results in this paper also provide a basis to the recently reported method for the determination of various aminothiols by indirect catalytic cathodic stripping voltammetry in the presence of $Ni^{2+}$ (refs[15,16]).

## EXPERIMENTAL

Most of the experimental details were reported elsewhere[1]. The background electrolyte consisted of $Na_2HPO_4$ and $CH_3COONa$ (0.024 mol $l^{-1}$ each) with 1 M $HClO_4$ added to adjust the pH. All the potential values are reported with respect to the SCE. In addition to the DC polarographic investigations, studies on the electrode–solution interface were done by non-phase selective AC polarography (60 Hz, 10 mV AC modulating voltage) and by recording drop time–potential curves. Some results are presented together with complex species distributions (Figs 2–5). Upper diagrams in these figures have the same abscissa axis as the lower ones.

## RESULTS AND DISCUSSION

### *Effect of Pen Concentration*

Figure 1 demonstrates the occurrence of the peak-shaped CNP in the presence of Pen (curve *2*, wave C; peak potential, –0.7 V). The decrease in the nickel diffusion current (wave A) in the presence of Pen is due to the inert character of the $[NiL_2]^{2-}$ species[1]. A further electrode process in this system is hydrogen evolution in the region of the catalytic hydrogen prewave D. The main characteristics of this wave were briefly described previously[1]; a detailed approach will be presented in a forthcoming paper.

The potential of the peak C is almost independent of the solution composition. In contrast, the peak current is strongly dependent on Pen concentration (Fig. 2a, curve *1*).

A comparison with the nickel species distribution (Fig. 2b) proves that the variation of the CNP current roughly parallels the change in [NiL] concentration. The hypothetical diffusion current of this species was computed using the Ilkovic constant for the free $Ni^{2+}$ ion[1] and was plotted as curve *2* in Fig. 2a. Although the computed values are somewhat higher than the expected ones (the diffusion coefficients of $Ni^{2+}$ should be higher than that of [NiL]), a comparison of curves *1* and *2* in Fig. 2a clearly demonstrates that the CNP current is much higher than the estimated diffusion current of [NiL]. This is a certain proof for the catalytic character of the wave C process. Consequently, this process should include a chemical step leading to the regeneration of the electrochemically active species, [NiL]. However, the regeneration step needs the

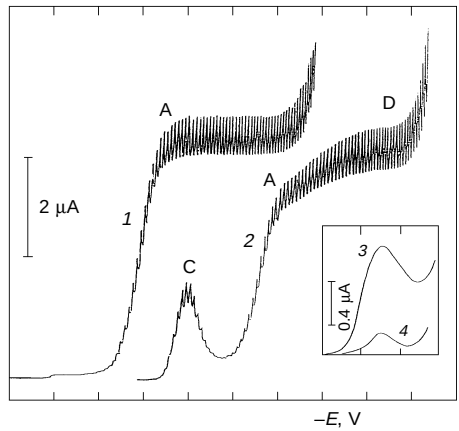


FIG. 1
Polarographic catalytic waves in the $Ni^{2+}$–Pen system at pH 6.52 and $[Ni^{2+}]_t$ = 1 mmol $l^{-1}$. [Pen]: *1* 0; *2* 0.48 mmol $l^{-1}$. Start potential –0.4 V; potential scale –0.2 V/division. Inset: a comparison of the Pen and Cys effects (0.2 mmol $l^{-1}$ each). *3* Cys; *4* Pen, pH 6.52, $[Ni^{2+}]_t$ = 2 mmol $l^{-1}$; the potential axis as before

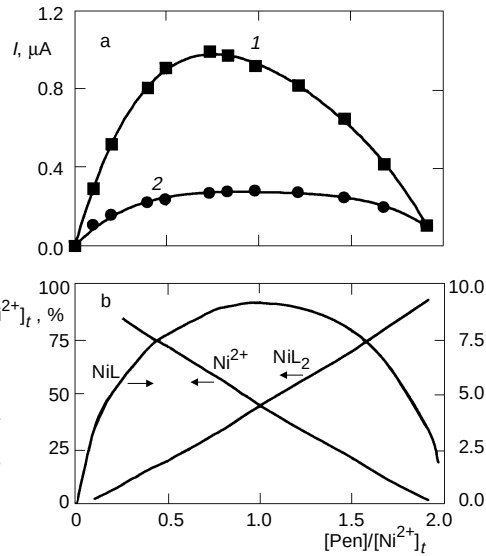


FIG. 2
Effect of the [Pen]/$[Ni^{2+}]_t$ ratio at constant $[Ni^{2+}]_t$ (0.6 mmol $l^{-1}$) and pH 6.52. a Wave C current; *1* experimental, *2* hypothetical diffusion current of [NiL]. b Nickel species distribution under the same conditions

presence of the free $Ni^{2+}$ ion as it results from the overlapping of curves *1* and *2* in Fig. 2a at a $[Pen]/[Ni^{2+}]_t$ ratio close to 2 ($[Ni^{2+}]_t$ stands for the overall $Ni^{2+}$ concentration). In this case, the concentration of the free $Ni^{2+}$ becomes very small and the $[NiL_2]^{2-}$ proportion approaches 100% of overall nickel concentration (Fig. 2b). In accord with its inert character[1], $[NiL_2]^{2-}$ species cannot supply nickel ion to the regeneration step and the CNP almost vanishes. The trend illustrated by curve *1* in Fig. 2a was also detected for other nickel concentrations (0.57 and 0.2 mmol $l^{-1}$) but, for the sake of simplicity, the relevant curves were not plotted in the figure.

The inset to Fig. 1 proves that, under similar conditions, cysteine (Cys, curve *3*) produces a much stronger catalytic nickel current than Pen does (curve *4*). This difference is certainly due to the masking of $Ni^{2+}$ by Pen in the form of the inert $[NiL_2]^{2-}$ complex; the analogous cysteine species is labile[1].

*Effect of Nickel Ion Concentration*

The effect of nickel concentration is displayed in Fig. 3 as a function of the $[Ni^{2+}]_t$ /[Pen] ratio at constant Pen concentration. CNP current was plotted as a function of this ratio for two different Pen concentrations (Fig. 3a), whereas the species concentration is plotted only for 0.2 mM Pen (Fig. 3b) to avoid complications. The species distribution for 0.5 mM Pen follows an analogous trend.

Two different regions can be distinguished in Fig 3, depending on whether the $[Ni^{2+}]_t$/[Pen] ratio is lower or higher than 1 : 2 (*i.e.*, the metal–ligand ratio in $[NiL_2]^{2-}$). For $[Ni^{2+}]_t$/[Pen] < 1 : 2, nickel is predominantly present as the $[NiL_2]^{2-}$ complex and an appreciable amount of free ligand (in the protonated form, $H_2L$) also exists (Fig. 3b).

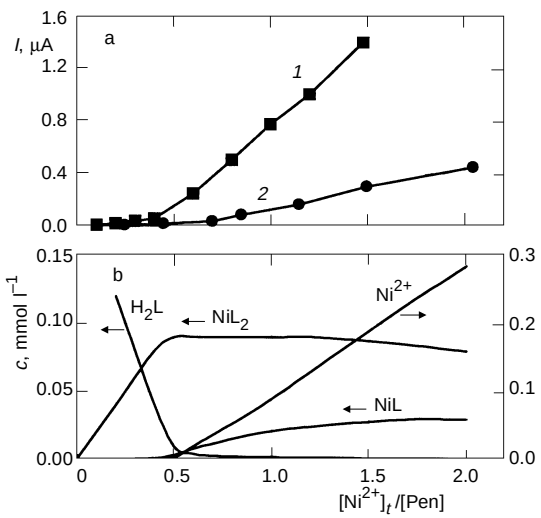


FIG. 3
Effect of the $[Ni^{2+}]_t$ /[Pen] ratio at pH 6.52. a CNP current; [Pen]: *1* 0.5 mmol $l^{-1}$, *2* 0.2 mmol $l^{-1}$. b Nickel species distribution at 0.2 M Pen

Under these conditions, the CNP current is extremely small (Fig. 3a) proving directly that $[NiL_2]^{2-}$ is not reducible and also it cannot dissociate as to provide reducible species ($Ni^{2+}$ or [NiL]).

If $[Ni^{2+}]_t$/[Pen] > 1 : 2, both free $Ni^{2+}$ ion and the [NiL] complex occur in the system in addition to $[NiL_2]^{2-}$, whereas the concentration of the free ligand ($H_2L$) becomes extremely low (Fig. 3b). Figure 3a demonstrates that the CNP current steadily increases under these conditions, mostly because of the increase in the concentration of the $Ni^{2+}$ ion. Indeed, with a reasonable accuracy, the CNP current is directly proportional to $Ni^{2+}$ concentration ($I$ (μA) = 0.07 + 1.564 $[Ni^{2+}]$ (mmol $l^{-1}$); $R^2$ = 0.996). Because $Ni^{2+}$ is reduced at more negative potentials ($E_{1/2}$ = –1.05 V, Fig. 1, curve *1*), it is clear that the species reduced in the potential range of the CNP is [NiL], whereas $Ni^{2+}$ takes part only in the chemical reaction which does regenerate the electroactive species. It is worth noting that the presence of the free ligand in the bulk of the solution is not essential for the occurrence of the CNP.

A comparison of Pen and Cys effects is shown in Fig. 4, where the results of EDTA titration at constant nickel concentration are recorded. Current values are therefore plotted in Fig. 4 as a function of free nickel concentration, computed as the difference between total nickel and added EDTA concentrations. Both nickel diffusion (squares) and CNP currents (circles) are plotted in this figure, in the presence of either Pen (a) or Cys (b). Diffusion current displays the usual trends in the Cys system, whereas, in the case of Pen, it assumes a linear increase only if the free nickel/Pen ratio exceeds 1 : 2 (*i.e.*, the metal/ligand ratio in the inert species $[NiL_2]^{2-}$). As far as the CNP induced by Pen is concerned, its dependence on the free nickel concentration shows the same trend as in Fig. 3a, with a very sharp transition from the region of zero current to the region of linear dependence on the free nickel concentration. As in Fig. 3, the transition point

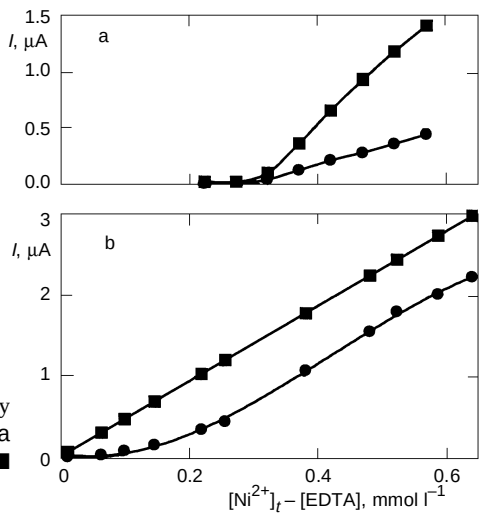


FIG. 4
Effect of free $Ni^{2+}$ concentration when varied by adding EDTA. $[Ni^{2+}]_t$ = 0.5 mmol $l^{-1}$; pH 7.11. a [Pen] = 0.5 mmol $l^{-1}$; b [Cys] = 0.5 mmol $l^{-1}$. ■ Wave A, ● wave C

corresponds to the metal/ligand ratio in bis(penicillaminato)nickel complex. In contrast, although present in the Cys system as well, such a transition occurs gradually because of the labile character of all complex species in this system (Fig. 4b).

In agreement with the inset to Fig. 1, data in Fig. 4 show that, under identical conditions, the CNP current induced by Pen is 4 to 5 times lower than that of Cys. EDTA titration also demonstrates that neither Pen nor Cys can displace EDTA in its nickel complex.

*Effect of pH*

As shown in Fig. 5a, the CNP current has significant values at pH > 4.5 only and, after a maximum at about pH 5.5, it falls to a small and almost constant value at pH > 6.5. The position of the maximum is slightly different for other Pen and $Ni^{2+}$ concentrations but roughly the same trend is observed under various conditions. A comparison of the curves in Figs 5a and 5b proves that the increase in the CNP current in the pH range 4.5–5.5 parallels the increase in the [NiL] concentration. The concentration of [NiL] remains almost unchanged at higher pH values and the current decrease could be ascribed to the decline in the $Ni^{2+}$ concentration owing to the formation of the inert $[NiL_2]^{2-}$ species. Actually, in the constant current region (pH > 6.5), both [NiL] and $Ni^{2+}$ concentrations are also independent of pH. In con-

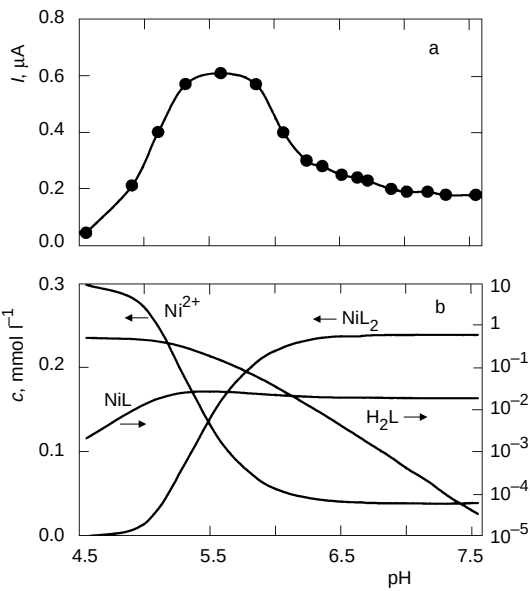


FIG. 5
a pH Effect on the CNP current; b species distribution as a function of pH. $[Ni^{2+}]_t$ = 0.3 mmol $l^{-1}$; [Pen] = 0.5 mmol $l^{-1}$

clusion, the maximum on the curve in Fig. 5a is due to two opposite effects of the pH increase: the increase in [NiL] concentration which is accompanied by a drop in the free $Ni^{2+}$ concentration.

*Effect of Interface Structure and Reactants Adsorption*

The effect of reactants adsorption was investigated by the method of electrocapillary curves and by non-phase-selective AC polarography (Fig. 6). Taking into account the electrode processes evidenced by DC polarography (curves *1′–3′*, Fig. 6), three different potential regions can be distinguished: the regions of the anodic mercury reaction ($E > -0.5$ V), the region of the CNP ($-0.5$ V $< E > -0.85$ V) and that of the diffusion-controlled nickel reduction ($E < -0.85$ V).

In the absence of $Ni^{2+}$, the formation of mercury(I) Pen thiolate (wave N on curves *2′* and *2″*) leads to the strong decrease in surface tension (curve *2*). Apparently, the anodic reaction occurs like in the case of Cys (ref.[17]). By analogy with that, it may be assumed that the more positive anodic wave, Q, involves an additional consumption of thiol[17,18]. An excess of $Ni^{2+}$ induces the increases in the surface tension (curve *3*) while shifting the anodic wave to more positive potentials (curves *3′*, *3″*, wave P), whereas the intensity of the wave decreases. In addition, wave Q vanishes in the presence of $Ni^{2+}$. Taking into account the equilibrium data in previous sections, this behaviour could be accounted for by the formation of the nickel–Pen complexes. Actually, under the conditions in Fig. 6, the concentration of free Pen is negligible in the presence of $Ni^{2+}$ and the single reactive species is [NiL]. The shift in the wave potential reflects the additional Gibbs energy required for the dissociation of this one before the formation of the mercury thiolate. Therefore, the overall anodic reaction in the presence of an excess of $Ni^{2+}$ can be formulated as follows:

$$2\,Hg \rightleftharpoons Hg_2^{2+} + 2\,e \qquad (A)$$

$$2\,[NiL] + Hg_2^{2+} \rightleftharpoons [Hg_2L_2] + 2\,Ni^{2+}\ . \qquad (B)$$

It is highly probable that the accumulation of Pen in catodic stripping voltammetry on the HMDE in the presence of a high excess of $Ni^{2+}$ (ref.[16]) occurs according to the above reactions.

Both the modification of the anodic wave N and the disappearance of the distorted wave Q are additional proofs of nickel blocking in the inert complex $[NiL_2]^{2-}$, which is the predominant nickel form. The adsorption of this negative species can also account for the change in the surface tension produced by $Ni^{2+}$ (curve *3*). On the other hand, the

removal of wave Q accounts for the change in the AC current on the positive side of the Faradaic peak P (curve *3″*). These data demonstrate that the $[NiL_2]^{2-}$ is inert towards nickel substitution by mercury as well. The competitive adsorption of $[NiL_2]^{2-}$ and the mercury(I) thiolate may account for the occurrence of the small maxima on curve *3* in the region of the anodic reaction. A more detailed discussion of the anodic reaction of Pen is beyond the scope of this paper.

It is still interesting to compare the above findings with data on the $Ni^{2+}$ effect on the mercury anodic reaction due to Cys (ref.[19]). In this case, a distinct anodic wave is produced by mercury oxidation followed by nickel substitution in the $[NiL_2]^{2-}$ complex. The absence of such an effect in the case of Pen (Fig. 6) is surely due to the inert character of the relevant $[NiL_2]^{2-}$ species.

The most important feature in the region of the CNP is a sharp decrease in the adsorption degree with the potential shift towards more negative value. This trend occurs both in the absence (curve *2*) or in the presence of $Ni^{2+}$ (curve *3*). Both the AC polarograms and the drop time–potential curves show that the adsorption is negligible at $E < -0.85$ V. The species adsorbed in the CNP region (which mostly lies on the negative side of the electrocapillary curve *3*) should be either neutral or positively charged and the most probable are [NiL] and $H_2L$. The shape of the CNP can therefore be accounted for by two opposite effects of potential shift towards more negative values. First, an increase in the rate constant of the charge-transfer reaction occurs, according to the Butler–Volmer

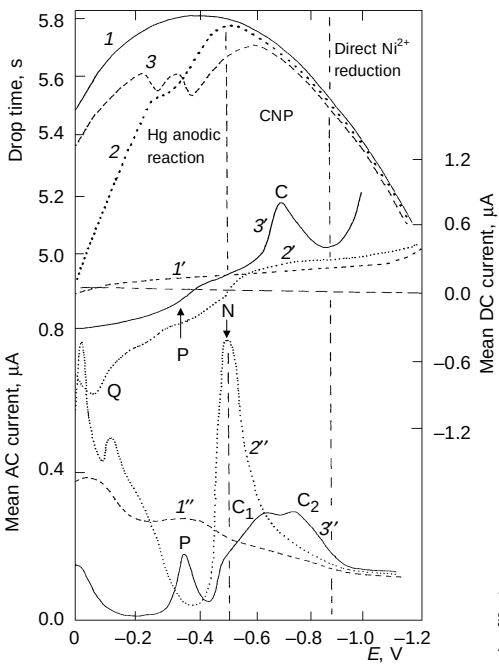


FIG. 6

*1–3* Electrocapillary curves; *1′–3′* DC polarograms; *1″–3″* AC polarograms. pH 6.52. [Pen] *1* 0, *2*, *3* 0.3 mmol $l^{-1}$. $[Ni^{2+}]_t$: *1*, *2* 0; *3* 0.56 mmol $l^{-1}$

relationship. Second, the concentration of the adsorbed reactant decreases owing to a decrease in the adsorption coefficient, according to the Frumkin theory[20].

Additional evidence for catalyst adsorption are provided by the effect of surfactants. CNP is strongly inhibited by both gelatine and tetrabutylammonium ion at trace level.

Although $[NiL_2]^{2-}$ is present within the whole potential range, its adsorption in the CNP region is apparently prevented by the negative charge and no inhibiting effects caused by this complex could be detected.

The shape of the AC polarogram $\mathcal{3}'$ in the CNP region and the first derivative of the DC polarogram $\mathcal{3}'$ are mostly alike. It could consequently be inferred that the AC current in the range of the CNP is chiefly due to the Faradaic process, with a negligible capacitance component. Conversely, the Faradaic AC current is negligibly small in the range of the nickel diffusion wave. According to the theory of AC polarography[21] it results that the standard rate constant for nickel reduction is much higher in the CNP region than in direct reduction of hydrated nickel ion.

Finally, the depression of the CNP noticed in the presence of alkali chlorides (in the sequence $Li^+ < Na^+ \leq K^+$) can be assigned to the decrease in $Ni^{2+}$ concentration at the boundary of the Helmholtz layer, due to the change in $\Psi$ potential. As a consequence, the rate of [NiL] regeneration becomes lower in this way. This is an additional evidence for the occurrence of this reaction at the electrode surface.

*Reaction Mechanism*

Figure 7 shows the main steps in nickel reduction catalyzed by Pen. According to data in previous sections, nickel ion exists in three different forms: free (hydrated) $Ni^{2+}$, [NiL] and $[NiL_2]^{2-}$. As previously shown[1], complexation by buffer components plays a minor role and can be neglected. The single reducible species in the CNP region is [NiL], which, in the bulk of the solution, is in equilibrium with free $Ni^{2+}$ (step I). $[NiL_2]^{2-}$ is in turn an inert complex[1] and does not take part in the electrode process. Because this species is extremely stable, CNP occurs only if $[Ni^{2+}]_t$/[Pen] > 1 : 2 so that both free $Ni^{2+}$ and [NiL] occur in significant concentrations. Under these conditions, the concentration of catalyst itself (*i.e.* free ligand) in the bulk of the solution is extremely low at pH > 6. Consequently, the catalytic cycle is initiated by the reduction of adsorbed [NiL] (step VI). In this way, some free catalyst molecules in adsorbed state are produced. The reducible species is thereafter regenerated (step VII) by reaction of the adsorbed catalyst with free nickel ion which is transported by diffusion from the bulk of the solution (step IV). Catalyst protonation (step VIII) could occur owing to relatively low pH values, but it does not bring about major kinetic complication as the proton transfer reaction involving usual Brönsted acids are known as being extremely fast[22].

The occurrence of the parallel regeneration reaction is proved by comparing the CNP current with the hypothetical diffusion current of [NiL] (Fig. 2a). Temperature effect

brings about an additional evidence for the kinetic control of the electrode process. Indeed, CNP current depends on temperature according to Arrhenius equation in the temperature range of 10–45 °C, with an apparent activation energy of 27 kJ $mol^{-1}$ (at pH 6.5, 2 . $10^{-4}$ M Pen and 6.5 . $10^{-4}$ M total $Ni^{2+}$).

The occurrence of nickel diffusion was proved by the effect of mercury column height (*h*). As long as CNP current is lower than 20% of the nickel diffusion current, the CNP height is independent of *h*. Conversely, the CNP current is a linear function of $h^{1/2}$ if it is higher than the above value but the intercept of current *vs* $h^{1/2}$ lines differs always from zero proving a partial diffusion control of the overall electrode process. The diffusing species responsible for this effect should be free $Ni^{2+}$ (step IV in Fig. 7) because [NiL] concentration is much lower.

A comparison of the CNP produced by Pen with that of Cys (Fig. 1) proves that in both cases the waves are alike in terms of peak potential and shape. This demonstrates that the nature of the electroactive center is identical in both cases. In other words, the [NiL]-type complex is also reduced in the $Ni^{2+}$–Cys system. The main difference between Pen and Cys systems, *i.e.* the intensity of the CNP, arises from the different kinetic stability of the $[NiL_2]^{2-}$ complexes. That with Cys is labile and its dissociation provides an additional amount of [NiL] which is reduced in the CNP process. Such a process is not possible in the Pen system because of the high inert character of the relevant $[NiL_2]^{2-}$ species (Fig. 7, step II). This characteristics leads to the blocking of both catalyst and metal ion in a proportion depending on the metal/ligand concentration ratio. Regeneration of [NiL] form by a parallel chemical reaction is therefore the single

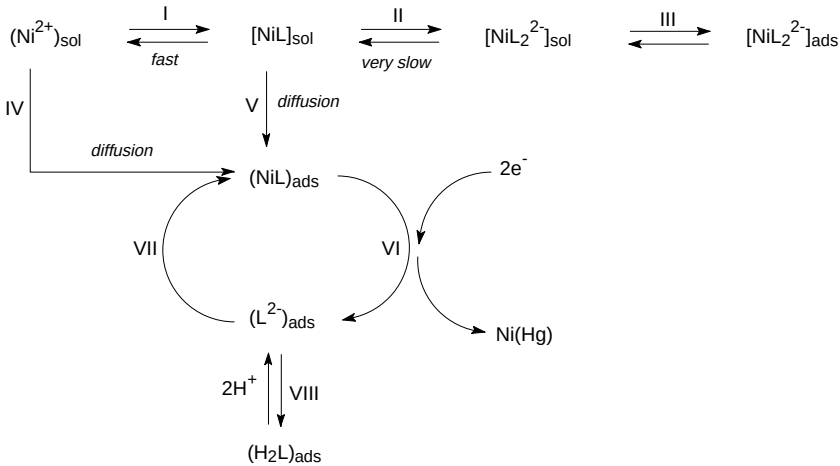


FIG. 7
Proposed reaction mechanism for nickel reduction catalyzed by Pen. The ligand in steps I and II was omitted for simplicity

way of providing the electrode process with the reducible species, in addition to the minor contribution of the [NiL] diffusion from the bulk of the solution (Fig. 7, step V). From this viewpoint, the catalytic nickel reduction in presence of Pen appears to be a simpler process compared with its Cys counterpart.

## CONCLUSIONS

Pen catalyzes the reduction of nickel ion producing a peak-shaped catalytic prewave at about –0.7 V *vs* SCE. The active species in the charge transfer reaction is (D-penicillaminato-*N*,*S*)nickel(II), [NiL], whereas the bis-ligand complex, $[NiL_2]^{2-}$, is both chemically and electrochemically inert. The above conclusion was derived from the correlation of the catalytic current with the nickel species distribution calculated under various conditions by means of available equilibrium data. It is interesting to note that the same stoichiometry of the active complex species was found in the case of cysteinyldipeptides by kinetic interpretation of electrochemical data under the assumption of diffusion-controlled catalyst adsorption[9]. A comparison of the peak potentials for the waves produced by either Pen or Cys suggests that the active species in the Cys system is the same kind of complex.

As the CNP is usually recorded in the presence of an excess of nickel ions, it results that the catalyst itself is present in the complex form. Therefore, the catalytic cycle is initiated by the reduction of the [NiL] species. The regeneration of that involves free nickel ions and adsorbed catalyst molecules released in the previous step.

An additional reaction path is possible in the case of Cys, where the dissociation of the labile $[NiL_2]^{2-}$ species can provide the reducible [NiL] form. Therefore, in this system the reaction mechanism could change from CE (at low $Ni^{2+}$/Cys ratios) to a process with parallel chemical reaction (at high $Ni^{2+}$/Cys ratios).

The strong dependence of the adsorption degree on the electrode potential brings about the typical bell-shaped form of the CNP. The neutral charge of [NiL] species precludes some important effect of $\Psi$ potential on the surface concentration of this species. The same applies to the free ligand, taking into account the neutral charge of the protonated form which is prevalent in the typical pH range. As far as $Ni^{2+}$ is concerned, a shift of $\Psi$ potential towards more negative values should produce an increase in its surface excess accompanied by the increase in the CNP current. As the CNP occurs near the potential of zero charge, this effect is very slight and does not overcome the influence of the potential on catalyst adsorption degree. Consequently, the peculiar shape of the CNP cannot be assigned to $\Psi$ potential effects on ionic reactants concentration in the double layer.

The results in this paper confirm the previous assumption on the reaction mechanisms in cathodic stripping voltammetry of Pen in presence of $Ni^{2+}$ (ref.[15]) as far as both preconcentration process and catalytic nickel reduction are concerned.

**REFERENCES**

1. Ion A., Banica F. G., Luca C.: *Collect. Czech. Chem. Commun.* **1998**, *63*, *187*.
2. Gergely A., Sovago I. in: *Metal Ions in Biological Systems* (H. Sigel, Ed.), Vol. 9, p. 77. Dekker, New York 1979.
3. Jones M. M., Basinger M. A., Weaver A. D.: *J. Inorg. Nucl. Chem.* **1981**, *43*, 1705.
4. Kuta J.: *Z. Anal. Chem.* **1966**, *216*, 243.
5. Banica F. G., Calusaru A.: *J. Electroanal. Chem.* **1983,** *145*, 389.
6. Banica F. G., Calusaru A: *J. Electroanal. Chem.* **1983,** *158*, 47.
7. Banica F. G., Diacu E.: *Collect. Czech. Chem. Commun.* **1991**, *56*, 140.
8. Calusaru A., Voicu V.: *J. Electroanal. Chem.* **1973,** *43*, 257.
9. Banica F. G.: *Talanta* **1985**, *32*, 1145.
10. Diacu E., Banica F. G., Ion I.: *Rev. Roum. Chim.* **1992**, *37*, 1389.
11. Diacu E., Banica F. G., Ion I.: *Rev. Roum. Chim.* **1993,** *38*, 1397.
12. Perrin D. D., Sayce J. G.: *J. Chem. Soc. A* **1968**, 53.
13. Halcrow M. A., Christou G.: *Chem. Rev.* **1994,** *94*, 2421.
14. Banica F. G.: *Bull. Soc. Chim. Fr.* **1991**, *128*, 697.
15. Ion A., Banica F. G., Fogg A. G., Kozlowski H.: *Electroanalysis* **1996**, *8*, 40.
16. Banica F. G., Fogg A. G., Ion A., Moreira J. C.: *Anal. Lett.* **1996**, *29*, 1415.
17. Heyrovsky M., Vavricka S.: *J. Electroanal. Chem.* **1997**, *423*, 125.
18. Heyrovsky M., Mader, P., Vavricka S., Vesela V., Fedurco M.: *J. Electroanal. Chem.* **1997**, *430*, 103.
19. Basinski A., Ceynowa J., Kuik M.: *Rocz. Chem.* **1963**, *37*, 1489.
20. Heyrovsky J., Kuta J.: *Principles of Polarography*, p. 296. Academic Press, New York 1966.
21. Smith D. E. in: *Electroanalytical Chemistry* (A. J. Bard, Ed.), Vol. 1, p. 1. Dekker, New York 1966.
22. Bell R. P.: *The Proton in Chemistry*, Chap. 8. Chapman and Hall, London 1973.